Drug Development and Industrial Pharmacy, 2009; 35(8): 959–968

informa
healthcare

ORIGINAL ARTICLE

Design of high payload PLGA nanoparticles containing melittin/sodium dodecyl sulfate complex by the hydrophobic ion-pairing technique

Linlin Yang[1], Fude Cui[1], Kai Shi[1], Dongmei Cun[1] and Rui Wang[2]

[1]*Department of Pharmaceutics, School of Pharmaceutical Science, Shenyang Pharmaceutical University, Shenyang, PR China and* [2]*Department of Pharmacology, School of Life Science and Biological Pharmacy, Shenyang Pharmaceutical University, Shenyang, PR China*

Abstract

The water-soluble peptide, melittin, was modified with an anionic agent, sodium dodecyl sulfate by hydrophobic ion-pairing. Investigations showed that the formed complex was very soluble in organic solvent, especially, in dimethylsulfoxide and dehydrated alcohol. Furthermore, the physiochemical properties of the complex in the solid state or in an aqueous medium were characterized using octanol/water partition measurement, Fourier transform infrared spectroscopy, and differential scanning calorimetry. The complex was formulated into poly(D,L-lactide–*co*-glycolide acid) nanoparticles by an emulsion solvent diffusion method. It was found that the nanoparticles of about 130 nm in size can be produced with a high encapsulation efficiency, and the entrapment of nanoparticles prepared with the formed complex increased from about 50% to nearly 100% compared with that for pure melittin. Moreover, the growth inhibitory effects of modified melittin and melittin-loaded nanoparticles in breast cancer MCF-7 cells were not changed comparing with free melittin as determined by (3-(4,5-dimethylthiazol-2-yl)-2,5-diphenyl tetrazolium bromide) assay.

Key words: *Complex; hydrophobic ion pairing; melittin; PLGA nanoparticles; SDS*

Introduction

With the development of biotechnology and genetic engineering, many pharmacologically active peptides and proteins are now good candidates for therapeutic drug treatment. However, their clinical applications involving oral administration have been limited because of their higher molecular weight (Mw) which makes absorption through biological membranes difficult, and their instability in the GI environment. Administration of therapeutic peptide drugs via the oral route is challenging. Many approaches have been used to deal with those problems, for example, employment of microparticle carriers such as nanoparticles[1–4], microemulsions, or liposomes[5–8]. It has been shown that M cells, which are located on the surface of Peyer's patches, are a possible pathway for transporting the nanoparticles through the gut epithelium[9,10]. In addition, the polymeric nature of nanoparticles protects the drug from adverse external conditions and controls its release[11–13].

Despite of the encouraging potential oral applications of biodegradable polymeric nanoparticles, formulation of water-soluble peptide drugs involving these carriers still presents a number of challenges. For example, the most widely used biodegradable polyesters, such as poly(lactic acid) (PLA), poly(glycolic acid) (PGA), and poly(D,L-lactide–*co*-glycolide acid) (PLGA), are not water soluble and this poses a significant challenge to encapsulating hydrophilic drugs into water-insoluble polymers efficiently[14,15]. The hydrophobic ion-pairing (HIP) technique has attracted great interest in the field of water-soluble protein/peptide delivery[16–18]. With the HIP technique, it is possible to increase the liposolubility of the protein by the complex formed[19–22], thereby increasing

Address for correspondence: Fude Cui, Department of Pharmaceutics, School of Pharmaceutical Science, Shenyang Pharmaceutical University, No. 103, Wenhua Road, Shenyang 110016, PR China. E-mail: lydia-mail@163.com

(Received 16 Jul 2008; accepted 31 Dec 2008)

ISSN 0363-9045 print/ISSN 1520-5762 online © Informa UK, Ltd.
DOI: 10.1080/03639040902718039

the solubility of more protein/peptides in organic solvents, and allowing homogenous mixing of the complex with water-insoluble polymers materials for encapsulating more protein/peptides[23,24]. Furthermore, for many proteins, this solution in organic solvents occurs with retention of their native structure and maintenance of their enzymatic activity[17]. Another possible advantage of the use of HIP is its ability to enhance the transport of proteins across the mucosal membranes[25,26].

In this study, melittin was used as a model drug to produce high entrapment PLGA nanoparticles using the HIP technique. Melittin, isolated from bee venom, is composed of 26 amino acids and is a highly hydrophilic polypeptide with a Mw of 2.86 kD[27]. Melittin is a typical representative of biologically active peptides with a high therapeutic potential. It has been found that melittin has a marked effect on the immune system[28], cardiovascular system[29], and blood[30] and exhibits anti-tumor activity[31]. It has been found that melittin can lead to cathepsis or necrosis of akaryocytes and labrocytes[32] and the anti-tumor activity of melittin could be associated with its effect on cellular membrane channels[33–35] or interference with cellular membranes[36,37]. However, the frequently used form for its clinical application is injection which is associated with temporary pain and a subsequent sustained increase in the skin temperature because of axon reflex. Therefore, there is a need for more suitable forms of administration. The biodegradable polymeric nanoparticles in a highly encapsulated form for oral administration are one of the most important choices.

In this study, melittin was combined with sodium dodecyl sulfate (SDS) via HIP to increase its lipophilicity. Octanol/water partition measurement, investigation of solubility, Fourier transform infrared (FTIR) spectroscopy, differential scanning calorimetry (DSC), and determination of MTT (3-(4,5-dimethylthiazol-2-yl)-2, 5-diphenyl tetrazolium bromide) were carried out to characterize the physiochemical properties and biological activity of the melittin/SDS HIP complex (Mel/SDS complex). In addition, the ion-paired complex dissolved in an appropriate organic solvent was directly formulated into PLGA nanoparticles based on the emulsion solvent diffusion method. The nanoparticles containing the Mel/SDS complex were characterized and compared with those containing free melittin.

Materials and methods

Materials

Melittin was isolated from natural bee venom (*Apis mellifera*) as described in the literature[38]. PLGA with weight average Mws of 10,050 and 9500, in which the copolymer ratio of D,L-lactide to glycolide was 75:25, were obtained from Chengdu Institute of Organic Chemistry, Chinese Academy of Sciences (Chengdu, China). SDS was purchased from Sigma-Aldrich (St. Louis, MO, USA). Polyvinyl alcohol (PVA) was supplied by Shin-Etsu Chemical Co., Ltd., Tokyo, Japan. MTT (3-(4,5-dimethylthiazol-2-yl)-2,5-diphenyltetrazolium bromide) was purchased from Sigma Chemical Co. (St. Louis, MO, USA). All other chemicals were of analytical grade.

Methods

Preparation of the melittin/sodium dodecyl sulfate complex

The Mel/SDS complex was prepared by the HIP technique. Melittin with a positive charge and SDS with a negative charge were combined by electrostatic attraction in aqueous solution. Briefly, melittin completely dissolved in acetate or phosphate buffer solution at various pH values was adjusted to a final concentration of 4 mg/mL. Various molar ratios of SDS dissolved in the same buffer solution against melittin from 0.1 to 1 were added to the melittin solution at room temperature and a cloudy precipitate was formed. After the solution was agitated at 500 rpm for 5 minutes, the cloudy solution was centrifuged at 10,000 rpm for 5 minutes at room temperature. When the SDS/melittin molar ratio was 6:1, the complexation reactions were also carried out at various temperatures and the effects of various agitation times on the complex formation were also investigated at room temperature. The white precipitates recovered were rinsed with deionized water and then freeze-dried.

Characterization of the melittin/sodium dodecyl sulfate complex

Determination of the amount of complexed melittin. The amount of melittin within the complexes was determined indirectly, that is, by measuring the amount of free melittin by the Lowry method[39] in the supernatant recovered after ultracentrifugation. The bonding efficiency (B.E.%) was expressed as the percentage melittin difference between the initial amount of melittin and the free amount in the supernatant relative to the total amount used for the complex preparation. The bonding efficiency was calculated as follows:

$$\text{B.E.\%} = \frac{(W_0 - W_s)}{W_0} \times 100, \quad (1)$$

where W_0 is the initial added amount of melittin and W_s is the amount of melittin in the supernatant.

Fourier transform infrared spectrophotometry and differential scanning calorimetry. FTIR spectrophotometry (FT-IR Spectrometer, BRUKER IFS-55, Switzerland)

was used to study the structure of melittin formed in the complex and the interaction between melittin and SDS. The infrared (IR) spectra of melittin, SDS, the complex, and a physical mixture of melittin and SDS were obtained by the KBr method.

The thermograms of melittin, SDS, Mel/SDS complex, and the Mel–SDS physical mixture were determined using DSC (stretching vibration DSC 60, Shimadzu Co., Kyoto, Japan). Approximately 3 mg of each sample was heated in aluminum pans from 30 to 300°C and scanning was carried out at 5°C/min.

Partitioning coefficient of the melittin/sodium dodecyl sulfate complex in a 1-octanol/water system. The shake-flask method was employed to determine the partitioning coefficient. In this, 2 mL of 1-octanol and 2 mL samples of various acetate or phosphate buffer solutions were added to the Mel/SDS complex (contained 1 mg melittin) or 1 mg free melittin. After 12 hours of agitation at room temperature, the mixture was centrifuged for 3 minutes at 2,000 rpm and, then, the concentration of melittin in the aqueous phase was measured by the Lowry method. The partition coefficient (P) was calculated as follows:

$$P = \frac{(C_0 - C_w)}{C_w}, \tag{2}$$

where C_0 is the initial concentration of melittin in the aqueous phase and C_w the final concentration of melittin in the aqueous phase.

Solubilization studies. Organic solvents with a range of polarity, such as dichloromethane (DCM), ethyl acetate (EAc), dimethylsulfoxide (DMSO), acetone, and dehydrated alcohol (EtOH), were used to evaluate the altered solubility of melittin after it was combined with SDS. Briefly, aliquots of organic solvent (1 mL) were added to the complexes and physical mixtures, followed by gentle vortexing for 5–10 minutes to produce an equilibrium system. The transmission of each system was recorded at 500 nm in a model 752 ultraviolet–visible spectrophotometer (Shanghai Spectrum Instruments Co., Ltd., Shanghai, China).

Preparation and characterization of nanoparticles. The PLGA nanoparticles containing free melittin or Mel/SDS complex were prepared by an emulsion solvent diffusion method. Briefly, 30 mg of PLGA and a selected amount of free melittin or Mel/SDS complex were dissolved in the organic solvents mixture. Two kinds of mixture were employed: a mixture of acetone (1.0 mL)/DMSO (0.3 mL) or acetone (1.0 mL)/EtOH (0.3 mL). The resultant polymer–drug solution was poured into 10 mL of PVA solution (1.0%, wt/vol) and the emulsified system was stirred at 500 rpm for 4 hours using a magnetic stirrer. The entire dispersed system was then centrifuged (40,000 × g for 30 minutes; CS 120GXL, Hitachi Co., Chiyoda, Tokyo, Japan) and resuspended in distilled water to remove the free drug and PVA. This process was then repeated and the resultant dispersion was freeze-dried, and the final product was stored at −20°C.

The loaded melittin within the nanoparticles was determined by a modified solvent dissolution method with DMSO[40]. Briefly, freeze-dried nanoparticles were accurately weighed (10–15 mg) and placed in a 10 mL flask to which 0.8 mL DMSO was added. After the nanoparticles had dissolved, 0.1 mol/L NaOH containing 0.5% SDS was added and gently mixed. After being allowed to stand at room temperature for 1 hour, the resultant solution became clear and the melittin concentration in the mixed solution was measured by the Lowry method. From this result, the percentage loading (wt/wt, melittin content per dry nanoparticles) was determined. Each sample was assayed in triplicate. The encapsulation efficiency was calculated based on the amount of melittin incorporated into the nanoparticles and the initial amount used. A small amount of freeze-dried nanoparticles was redispersed in distilled water and their size was measured by laser diffraction using a Coulter LS 230 instrument (Beckman Coulter Co., Ltd., Miami, FL, USA). The diameters were measured by using the volume-based distribution.

Bioactivity. The growth inhibitory effects of free melittin, Mel/SDS complex, and melittin in nanoparticles in breast cancer MCF-7 cells were measured by MTT assay. Briefly, cells were seeded onto 96-well plates at 2×10^4 cells/mL per well and then allowed to adhere and spread for 24 hours. The freeze-dried nanoparticles (entrapment efficiency: 92.6 ± 4.6%) loaded with Mel/SDS complex were dispersed in 2 mL physiological saline, and the system was shaken at 50 rpm at 37°C. After 2 hours, the supernatant was collected by ultracentrifugation and the amount of melittin released from the nanoparticles was determined by the Lowry method. Then, a selected volume of the supernatant with defined amount of melittin was freeze-dried. Selected amounts of free melittin, Mel/SDS complex, and melittin released from nanoparticles were dissolved in phosphate buffered saline (PBS) (containing a trace of DMSO or alcohol). Various concentrations of the compounds were then added and cultured for another 4 days at 37°C. Then, 20 μL of 5 mg/mL MTT solution was added to each well and incubated for 4 hours. After this, the medium was removed and the cells were dissolved in 200 μL DMSO for 10 minutes at room temperature. The absorbance at 570 nm was measured using a 96-well microtiter plate reader. Growth inhibition was determined by comparison with untreated cells (%) and the drug concentration that inhibited the cell growth by a half (GI_{50}) was calculated.

Results and discussion

Effect of pH and the molar ratio (sodium dodecyl sulfate to melittin) on the amount of complexed melittin

Melittin is a 26-amino acid peptide with six basic amino groups .The sequence is Gly–Ile–Gly–Ala–Val–Leu–Lys–Val–Leu–Thr–Thr–Gly–Leu–Pro–Ala–Leu–Ile–Ser–Trp–Ile–Lys–Arg–Lys–Arg–Gln–Gln[41,42]. The p*I* value of melittin is 12.06[43] and, below the p*I* value (pH 4.0, 7.0, and 9.0), melittin is always positively charged. Therefore, it is easy for melittin to bind to the negatively charged sulfate groups of SDS. As seen in Figure 1, the Mel/SDS complex formed was insoluble and white precipitates were formed, which also showed that the positively charged melittin can be stoichiometrically ion-paired with the negatively charged SDS. This is in good agreement with the findings reported previously that complex precipitates can be formed between SDS and a number of proteins, such as lysozyme, conalbumin, insulin, and ovalbumin[16,20,24,44]. The fraction of complexed melittin was determined by measuring the amount of precipitated melittin in the solution after centrifugation. In this study, it was found that the molar ratio of SDS to melittin had great influence on the amount of complexed melittin. However, the temperature and reaction time had little effect (Figure 1). As shown in Figure 1, the bonding efficiencies at 30 or 40°C were not significantly different from that at 20°C (*t*-test both $P>0.1$) and, after agitating for 5 minutes, the bonding efficiency was similar for all (*t*-test both $P>0.1$). It was found that up to 98% of the melittin formed a compound with SDS when the molar ratio of melittin to SDS was 1:6. In other words, when one molecule of melittin formed a compound with six molecules of SDS, the complex formed was very stable and exhibited a high degree of hydrophobicity. This may be related to how many charges were presented by melittin. Melittin has 26 amino acid residues, six of which are positively charged, and there are no negative charges over the pH range studied[45,46]. At pH 4.0, 7.0, and 9.0, melittin always carries six positive charges. However, obviously, before we obtained the highest bonding efficiency, when the molar ratio was greater than 2:1, the bonding efficiency of melittin at pH 7.0 and 9.0 was higher than that when precipitation occurred at pH 4.0. Melittin gradually becomes more electropositive as the pH value shifts away from its p*I* value, then it is easy to attract negatively charged groups. We expected that the complex would be more easily formed at pH 4.0, initially, assuming that pK_a value of sulfate group in SDS is less than 4. However, Figure 1 shows unexpected results. This homoioplastic behavior has also been observed by others[24]. As the pH approaches the p*I* value of melittin, the hydrophobic interaction between melittin molecules became more intense, causing the surface-neutralized melittin to interact with active molecules by a nonspecific hydrophobic interaction during the formation of a precipitate in addition to the ion-pairing action[47]. It was also interesting to note that, after reaching the highest bonding efficiency (1:6, melittin/SDS molar ratio), addition of an excess of SDS to the insulin solution reduced the bonding efficiency. The solution eventually turned clear and the bonding efficiency was 0% at an SDS/melittin molar ratio of 10 (Figure 1). Upon further addition of excess SDS beyond the point of highest bonding efficiency, the additional SDS in the solution then formed micelles, and the water-insoluble Mel/SDS complex tended to dissociate in the micelles. This reverse ion-pairing behavior has also been observed by using other proteins or peptides with different complexing agents, such as fatty acids, surfactants, and phospholipids[16,19,47,48].

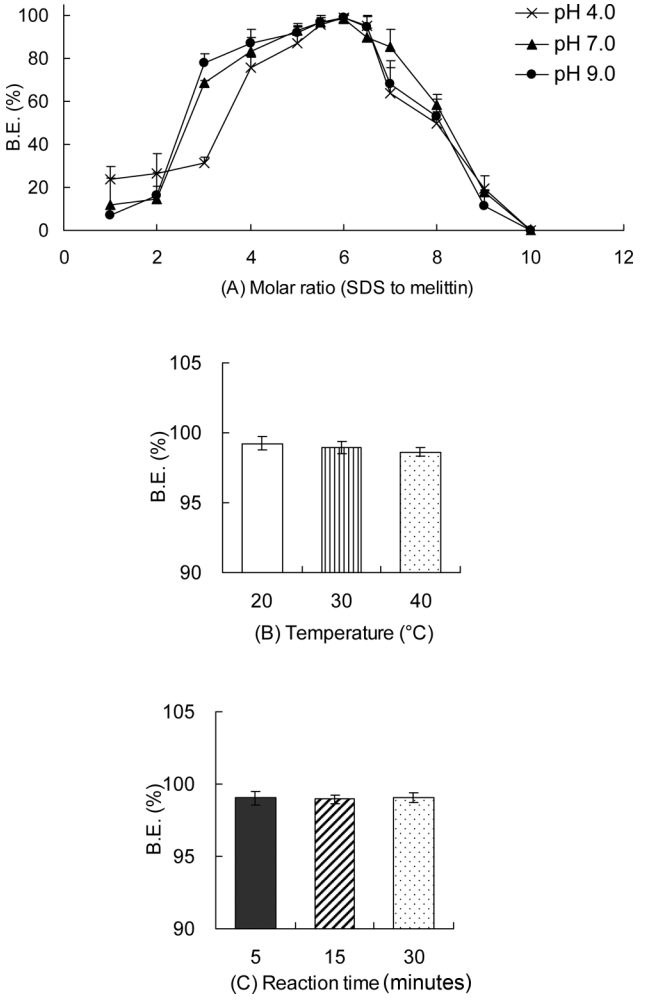

Figure 1. Bonding curve of SDS to melittin: (A) the effect of different SDS/melittin molar ratios on the bonding efficiency; (B) the effect of different temperatures on the bonding efficiency; and (C) the effect of different reaction times on the bonding efficiency (mean ± SD, $n = 3$).

The Mel/SDS complex (1:6, molar ratio) was used in the subsequent studies.

Infrared spectra analysis

The structure of the Mel/SDS complex was studied by IR spectroscopy to examine whether the native structure of the protein was retained in the complex. The IR spectra of melittin, SDS, their physical mixture and the complex are shown in Figure 2. In the melittin spectrum (Figure 2C), three main bands were observed at 3311.6 (amide A band), 1652.9 (amide I), and 1539.8 (amide II)[49,50]. It was also shown that four distinctive features at 2918.7, 2850.3, 1219.7, and 1083.9 cm^{-1} were IR absorption bands corresponding to the CH_2 asymmetric, CH_2 symmetric, SOO^- asymmetric, and SOO^- symmetric stretching vibration modes in the SDS spectrum (Figure 2D)[51]. This showed that the amide I band (1630–1700 cm^{-1}) of the complex and pure melittin, a characteristic area widely used as an indication for the secondary structure (backbone) conformation of protein/peptides[52], was similar. This suggested that the secondary structural conformation of melittin in the complex was unchanged. The spectrum of the physical mixture had the distinctive features of both melittin and SDS.

However, there was a difference between the physical mixture and the complex in their IR spectra (Figure 2A–B). The distinctive feature in the Mel/SDS complex corresponding to the β_{N-H} sheet at 1540.1, 1541.9 cm^{-1} decreased, and the peak intensity of the band at 1390–1330 cm^{-1}, corresponding to N—O-stretching, increased. Comparing the complex with SDS in the IR spectra (Figure 2A and D), the characteristic absorption band at 1219.7 cm^{-1} in the SDS spectrum corresponding to S—O—H stretching was less marked and shifted to the low field in the complex spectrum, which suggests that there were interactions between the NH^+ of the protein and the SOO^- of SDS during complex formation[16]. In addition, no new peaks were observed in the mixture

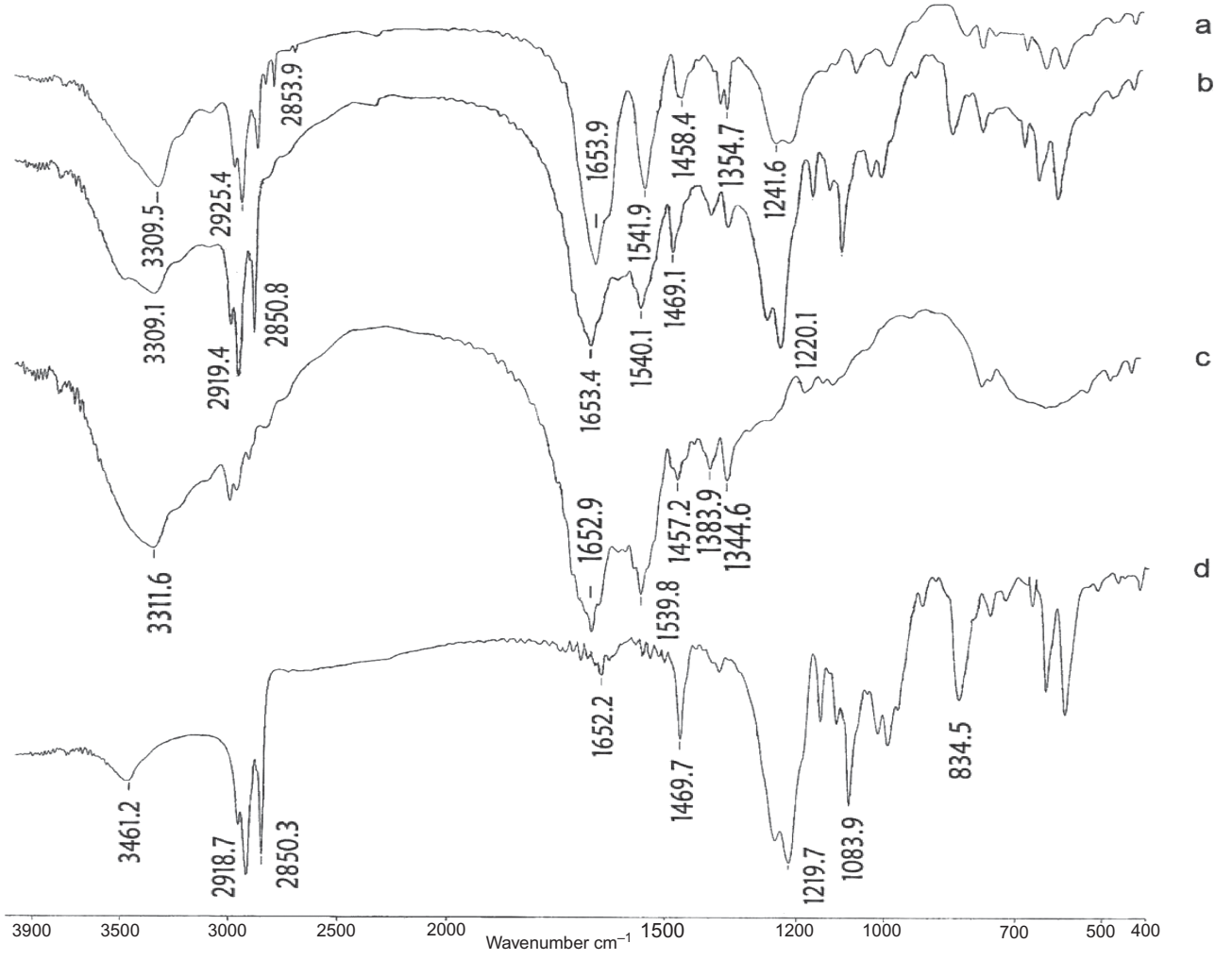

Figure 2. Infrared spectra of (A) Mel/SDS complex (1:6, molar ratio); (B) melittin and SDS physical mixture; (C) melitin; and (D) SDS.

and complex. These observations suggest that some weak physical interactions between melittin and SDS take place during formation of the complex.

Differential scanning calorimetry measurement

DSC was employed to investigate the Mel/SDS complex formed in this study. DSC curves of melittin, SDS, Mel/SDS complex, and the Mel–SDS physical mixture are shown in Figure 3. The endothermic peaks of SDS were observed at 95.11, 188.60, 203.59, and around 250°C, respectively. The Mel–SPC physical mixture also had an endothermic peak at 93.89, 188.98°C. and a broad endothermic peak at around 230°C. However, no melting point peak was found in the curve of native melittin. We suggest that melittin was in a high-energy amorphous state. The Mel/SDS complex showed a broad endothermic peak at 130.24, 184.15, and about 280°C. The endothermic peaks of SDS became smaller and broader. The changes in the low temperature band correspond to the thermodynamic transformation of the crystal structure from an orderly to a disorderly form[53]. As shown in Figure 3, there was a broad and small endothermic peak at 184.15°C in the curve of the complexes and a sharp endothermic peak at 188°C in the curve of SDS, both of which suggested that the intramolecular ion interaction of SDS in the complexes was weaker and more disorderly than that in pure SDS. This may be associated with the occurrence of an intermolecular ion interaction between SDS and melittin. The difference was interpreted as an interaction between the melittin and SDS and the formation of the Mel/SDS complex[54]. Above 200°C, there were broad and large peaks in the curve of the complex. According to the theory of heat denaturation of proteins[55,56], this result indicates that at such a high temperature, the spatial structure of the protein might be disrupted because of the weak ionic interaction between melittin and SDS[57]. Furthermore, the endothermic peaks of the physical mixture became smaller. This suggests that some SDS could fuse with melittin during the heating procedure.

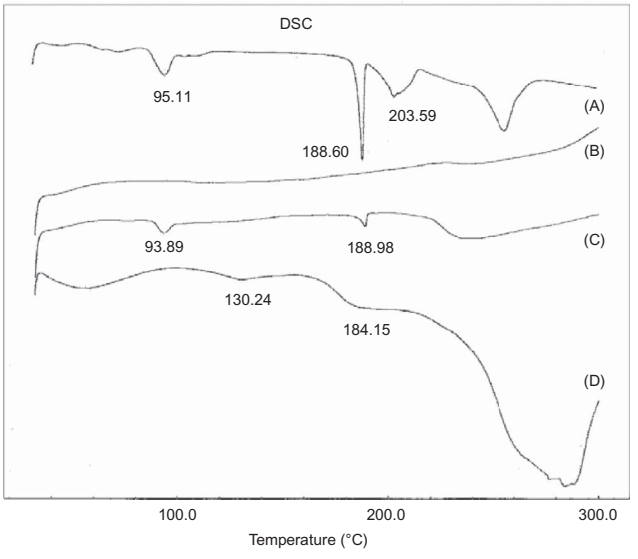

Figure 3. DSC curves of (A) SDS; (B) melitin; (C) melitin and SDS physical mixture (1:6, molar ratio); and (D) Mel/SDS complex (1:6, molar ratio).

Partition coefficient and solubilization of the melittin/sodium dodecyl sulfate complex in organic solvents

It was expected that the aqueous solubility of melittin would decrease after complex formation. In order to confirm the increased lipophilicity of the complex, its partition coefficient in 1-octanol/buffer was measured (as shown in Table 1). As a control, the partition coefficient of pure melittin was also measured. Compared with that of pure melittin, the partition coefficient of the complex increased markedly in the three buffer systems. The lipophilicity of melittin was increased by the hydrophobic agent, SDS, in the complex[58]. In addition, both the partition coefficients of the complex and pure melittin in pH 7.0 buffer were higher than that in the other two buffer systems (pH 4.0 and 9.0). This may be attributed to the increased hydrophobic interaction between melittin molecules as the pH approaches the p*I* value of melittin. These results are in good agreement with the findings involving the pH effects on Mel/SDS complex formation.

As shown in Table 1, the ability of the Mel/SDS complex formed by HIP to reduce the aqueous solubility of melittin has been confirmed. Furthermore, it was found that the solubility of melittin in organic media increased after the formation of the Mel/SDS complex (Figure 4). We chose five of the most frequently used organic solvents as the emulsion solvents in the diffusion method to be investigated. They were DCM, EAc, ethyl alcohol (EtOH), acetone, and DMSO. The transmittance of the organic solvent solution (except DCM) with the complex was higher than 70%, especially in DMSO and EtOH. When the Mel/SDS complex was dissolved in DMSO and EtOH, the transmittance of the system increased up to about 100%, which indicated that melittin was completely dissolved in the organic phase. As a control, the transmittance of melittin and the SDS physical mixture was no more than 60%,

Table 1. Partition coefficients of Mel/SDS complex (1:6, molar ratio) and melittin in 1-octanol/buffer (Mean ± SD, $n = 3$).

	Mel/SDS complex		Pure melittin	
	P	log P	P*	log P*
pH 4.0	11.79 ± 2.50	1.07 ± 0.09	0.21 ± 0.08	−0.69 ± 0.19
pH 7.0	29.39 ± 4.78	1.46 ± 0.07	0.52 ± 0.08	−0.29 ± 0.07
pH 9.0	20.51 ± 2.14	1.31 ± 0.04	0.19 ± 0.05	−0.74 ± 0.11

*t-test, $P < 0.01$.

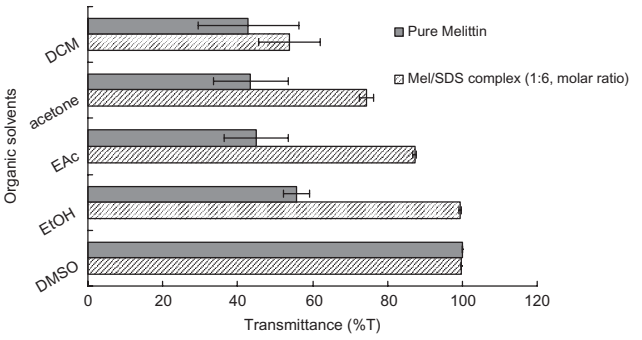

Figure 4. The solubility of melittin in different organic solvents (mean ± SD, $n = 3$).

which demonstrated that Mel/SDS complex enhances the solubility of melittin in organic solvents. It was also observed that the transmittance of the organic solvent solution with different polarities was also different. In other organic solvents (acetone, EAc, DCM), the transmittance was not so high. The polarity of those organic solvents was in the order: DMSO > EtOH > EAc > acetone > DCM. It is known that the agents were reconnected to the HIP complex mainly via ionic attraction[17,18,24,48,59]. Thus, the difference may be attributed to the strong polarity of DMSO and EtOH, which can reduce the ionic attraction in the complex and produce ionic solvation, leading to the dissolution of melittin in organic solvents[60].

Preparation and characterization of nanoparticles

Using the HIP technique, the increased solubility of melittin in organic solvents enabled nanoparticles encapsulated with melittin to be prepared with a high entrapment efficiency (shown in Table 2). About 50% of pure melittin was loaded into the PLGA nanoparticles, whereas nearly 100% of the initially added Mel/SDS complex was loaded. As shown in Table 2, the size distribution of nanoparticles was measured as a function of the initial amount of melittin added to the nanoparticles. The solubility of the Mel/SDS complex both in DMSO and EtOH was good. The size of nanoparticles prepared with the DMSO and acetone mixture was similar to that prepared with the EtOH and acetone mixture, although the entrapment efficiency of the nanoparticles prepared with DMSO was less than that prepared with EtOH. This may be because of the slow spreading rate of DMSO in the aqueous phase. The spreading rate of DMSO in the aqueous phase was slower than that of EtOH. Thus, the Mel/SDS complex dissolved in DMSO had a greater chance to escape from entrapped polymer materials during diffusion of the organic phase and the polymer forming nanoparticles. It was shown that the amount of melittin loaded in nanoparticles was about 6% and the entrapment efficiency was high (about 90%). In addition, nanoparticles as small as about 130 nm in diameter could be successfully prepared. It is also observed that the entrapment efficiency of melittin was reduced from 99.6 ± 1.7% to 54.8 ± 3.1% on increasing the amount of melittin loaded in nanoparticles from 3.87 ± 0.13% to 7.08 ± 0.40%. In addition, the size of the nanoparticles increased slightly from 128 to 141 nm. The increase in the unit volume of melittin might cause an increase in the probability of leakage of melittin from polymer materials. Thus, even though the amount of melittin loaded in nanoparticles increased, the entrapment efficiency was reduced. Nevertheless, the viscosity of the organic phase increased as the initial added amount of the Mel/SDS complex increased. The size increment was likely caused by the viscosity effect of the organic phase. As shown in Figure 5, the size distribution of the nanoparticles prepared with the Mel/SDS complex (entrapment efficiency: 92.6 ± 4.6%) was narrow and was mainly about 130 nm.

Activity

The growth inhibitory effects of melittin, Mel/SDS complex, and melittin released from nanoparticles in MCF-7 cells were determined by MTT assay. The drug concentration that inhibited half the cell growth (GI_{50}) was calculated. In this study, the growth inhibitory effects of various concentrations (1.25, 2.5, 5.0, 10.0, 20.0, and 40.0 μg/mL) of melittin or a melittin-equivalent dose (in the complex) were investigated (Figure 6). As shown in Figure 6, the GI_{50} of free melittin, the complex, and melittin released from nanoparticles were 3.64 ± 0.66, 3.92 ± 0.52, and 4.42

Table 2. Characterization of PLGA nanoparticles prepared with pure melittin and Mel/SDS complex (1:6, molar ratio) (mean ± SD, $n = 3$).

Drug added	Oil phase	W_p (mg)	W_m (mg)	Melittin loading (wt/wt, %)	Entrapment efficiency (%)	Particle yield (%)	Diameter (nm)
Pure melittin	DMSO/acetone	30	1	1.87 ± 0.20	49.3 ± 5.2	84.9 ± 2.0	112 ± 29
Complex	DMSO/acetone	30	1	3.17 ± 0.12	87.0 ± 5.6	87.8 ± 2.4	124 ± 21
Complex	EtOH/acetone	30	1	3.87 ± 0.13	99.6 ± 1.7	81.4 ± 4.0	128 ± 17
Complex	EtOH/acetone	30	2	6.36 ± 0.32	92.6 ± 4.6	87.6 ± 5.4	134 ± 18
Complex	EtOH/acetone	30	3	6.99 ± 0.43	70.0 ± 4.1	86.4 ± 2.4	137 ± 18
Complex	EtOH/acetone	30	4	7.08 ± 0.40	54.8 ± 3.1	84.9 ± 1.8	141 ± 19

W_p is the initial amount of PLGA added and W_m is the initial amount of melittin added.

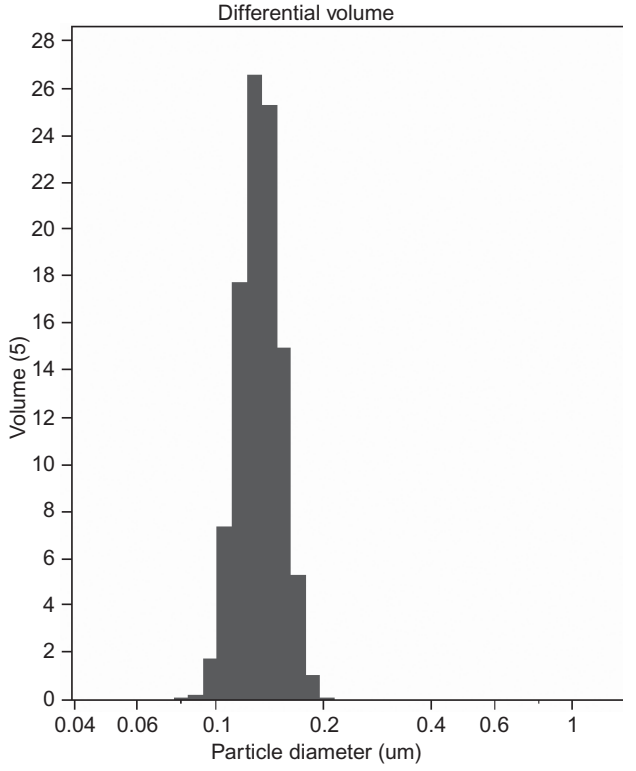

Figure 5. Size distribution of the nanoparticles (entrapment efficiency: 92.6 ± 4.6%) prepared with the Mel/SDS complex (1:6, molar ratio).

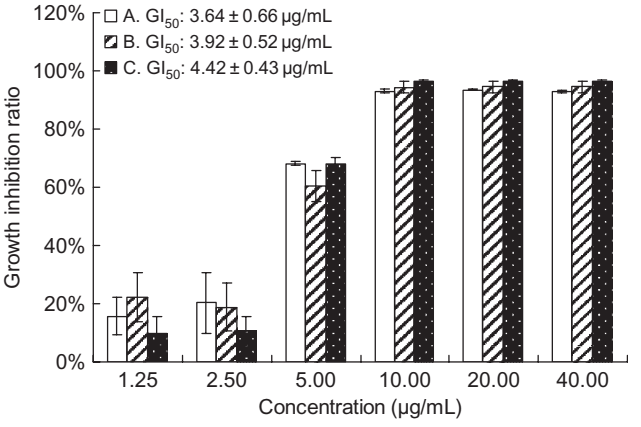

Figure 6. The growth inhibition ratios of various concentrations of melittin in breast cancer MCF-7 cells. (A) Free melittin; (B) melittin in Mel/SDS complex (1:6, molar ratio); and (C) melittin released from nanoparticles (entrapment efficiency: 92.6 ± 4.6%) (mean ± SD, $n = 3$).

± 0.43 μg/mL, respectively. The GI_{50} of the complex and melittin released from nanoparticles were not significantly different from that of free melittin (*t*-test both $P > 0.1$). These data clearly indicate that the melittin in the complex retained its bioactivity in vitro, which was consistent with the results showing that the protein retained its native structural integrity in the HIP complex which has been confirmed by other studies. After preparation of nanoparticles containing Mel/SDS complex, the melittin in the nanoparticles also retained its bioactivity in vitro.

Conclusions

In this article, the melittin–sodium lauryl sulfate complex was prepared by the HIP technique. Compared with that of uncomplexed melittin, the partition into 1-octanol in an octanol/water system and the solubility in organic solvents of the complexed melittin were significantly increased. After complex formation with SDS, melitin was successfully formulated into biodegradable nanoparticles by the emulsion solvent diffusion method. The complex with loaded nanoparticles, characterized by a high drug entrapment efficiency (about 90%) and drug content (6–7%), was obtained by the novel HIP strategy. In addition, the bioactivities of melittin in the complex and in the nanoparticles were similar to those of free melittin, as verified by in vitro anti-tumor testing.

Declaration of interest: The authors report no conflicts of interest.

References

1. Allaouiattarki K, Fattal E, Pecquet S, Trolle S, Chachaty E, Couvreur P, et al. (1998). Mucosal immunogenicity elicited in mice by oral vaccination with phosphrylcholine encapsulated in poly(D,L-lactide-coglycolide) microspheres. Vaccine, 16:685–91.
2. Araujo L, Sheppard M, Lobenberg R, Kreuter J. (1999). Uptake of PMMA nanoparticles from the gastrointestinal tract after oral administration to rats: Modification of the body distribution after suspension in surfactant solutions and in oil vehicles. Int J Pharm, 176:209–44.
3. Bowersock TL, HogenEsch H, Suckow M, Guimond P, Martin S, Borie D, et al. (1999). Oral vaccination of animals with antigens encapsulated in alginate microspheres. Vaccine, 17:1804–11.
4. Hussain N, Jani PU, Florence AT. (1997). Enhanced oral uptake of tomato lectin conjugated nanoparticles in the rat. Pharm Res, 14:613–8.
5. Kato Y, Hosokawa T, Ito K. (1993). Influence of liposomes on tryptic digestion of insulin. Biol Pharm Bull, 16:457–61.
6. Lee VHL, Yamamoto A, Kompella UB. (1991). Mucosal penetration enhancers for facilitation of peptides and protein drug absorption. Crit Rev Ther Drug Carrier Syst, 8:91–192.
7. Liu X, Chen D-W, Xie L-P, Zhang R-Q. (2003). Oral colon-specific drug delivery for bee venom peptide: Development of a coated calcium alginate gel beads-entrapped liposome. J Control Release, 93:293–300.
8. Muramatsu K, Maitani Y, Takayama K, Nagai T. (1999). The relationship between the rigidity of the liposomal membrane and the absorption of insulin after nasal administration of liposomes modified with an enhancer containing insulin in rabbits. Drug Dev Ind Pharm, 25:1099–105.
9. Clean SM, Prosser E, Meehan E, Malley DO, Clarke N, Ramtoola Z, et al. (1998). Binding and uptake of biodegradable poly-D,L-lactide micro and nanoparticles in intestinal epithelia. Eur J Pharm Sci, 6:153–63.

10. Jung T, Kamm W, Breitenbach A, Kaiserling E, Xiao JX, Kissel T. (2000). Biodegradable nanoparticles for oral delivery of peptides: Is there a role for polymers to affect mucosal uptake. Eur J Pharm Biopharm, 50:147–60.
11. Romero-Cano MS, Vincent B. (2002). Controlled release of 4-nitroanisole from poly(lactic acid) nanoparticles. J Control Release, 82:127–35.
12. Sakuma S, Suzuki N, Kikuchi H, Hiwatari K, Arikawa K, Kishida A, et al. (1997). Oral peptide delivery using administered salmon calcitonin by polystyrene nanoparticles having poly(*N*-isopropylacrylamide) branches on their surfaces. Int J Pharm, 158, 69–78.
13. Takeuchi H, Yamomoto H, Kawashima Y. (2001). Mucoadhesive nanoparticulate systems for peptide drug delivery. Adv Drug Deliv Rev, 47:39–54.
14. Niwa T, Takeuchi, H, Hino T, Kunuo N, Kawashima Y. (1994). In vitro drug release behaviour of D,L-lactide/glycolide copolymer (PLGA) nanospheres with nafarelin acetate prepared by a novel spontaneous emulsification solvent diffusion method. J Pharm Sci, 83:727–32.
15. Park TG, Lu W, Crotts G. (1995). Importance of in vitro experimental conditions on protein release kinetics, stability and polymer degradation in protein encapsulated poly(D,L-lactic-co-glycolic acid) microspheres. J Control Release, 33:211–22.
16. Dai WG, Dong LC. (2007). Characterization of physiochemical and biological properties of an insulin/lauryl sulfate complex formed by hydrophobic ion pairing. Int J Pharm, 336:58–66.
17. Meyer JD, Mark MC. (1998). Hydrophobic ion pairing: Altering the solubility properties of biomolecules. Pharm Res, 15:188–93.
18. Quintanar-Guerrero D, Allemann E, Fessi H, Doelker E. (1997). Applications of the ion-pair concept to hydrophilic substances with special emphasis on peptides. Pharm Res, 14:119–27.
19. Adjei A, Rao S, Garren J, Menon G, Vadnere M. (1993). Effect of ionpairing on 1-octanol–water partitioning of peptide drugs. I: The nonapeptide leuprolide acetate. Int J Pharm, 90:141–9.
20. Matsuura J, Powers ME, Manning MC, Shefter E. (1993). Structure and stability of insulin dissolved in 1-octanol. J Am Chem Soc, 115:1261–4.
21. Paradkar VM, Dordick JS. (1994). Mechanism of extraction of chymotrypsin into isooctane at very low concentrations of aerosol OT in the absence of reversed micelles. Biotechnol Bioeng, 43:529–40.
22. Powers ME, Matsuura J, Brassell J, Manning MC, Shefter E. (1993). Enhanced solubility of proteins and peptides in nonpolar solvents through hydrophobic ion pairing. Biopolymers, 33:927–32.
23. Falk R, Randolph TW, Meyer JD, Kelly RM, Manning MC. (1997). Controlled release of ionic compounds from poly(L-lactide) microspheres produced by precipitation with a compressed antisolvent. J Control Release, 44:77–85.
24. Yoo HS, Choi HK, Park TG. (2001). Protein–fatty acid complex for enhanced loading and stability within biodegradable nanoparticles. J Pharm Sci, 90:194–201.
25. Bradshaw JP. (1997). Phophatidylglycerol promotes bilayer insertion of salmon calcitonin. Biophys J, 72:2180–96.
26. Dua R, Duncan M, Zia H, Needham TE. (1998). The influence of the enhancer dimyristoylphosphatidylglycerol and formulation factor on the nasal absorption of salmon calcitonin. Drug Deliv, 5:127–34.
27. Angelika N, David AT. (2001). Self-association and membrane-binding behavior of melittins containing trifluoroleucine. J Am Chem Soc, 123:7407–13.
28. Jutel MN, Pichler WJ, Skribic D, Urwyler A, Dahinden C. (1995). Bee venom immunotherapy results in decrease of IL-4 and IL-5 and increase of IFN-gamma secretion in specific allergen-stimulated T cell cultures. J Immunol, 154:4187–94.
29. Thomas GR, Hiley CR. (1988). Cardiovascular effect of intracerebroventricular bradykinin and melittin in the rat. J Pharm Pharmacol, 40:721–3.
30. Pogliani EM, Cofrancesco E. (1983). Thrombotic thrombocytopenic purpura. Haematologica, 68:546–57.
31. Liu X, Chen D-W, Xie L-P, Zhang R-Q. (2002). Effect of honey bee venom on proliferation of K1736M2 mouse melanoma cell in-vitro and growth of murine B16 melanomas in-vivo. J Pharm Pharmacol, 54:1–8.
32. Lo WC, Henk WG, Enright FM. (1997). Light-microscopic studies of 3T3 cell plasma membrane alterations mediated by melittin. Toxicon, 35:15–26.
33. Laine RO, Morgan BP, Esser AF. (1988). Comparison between complement and melittin hemolysis: Anti-melittin antibodies inhibit complement lysis. Biochemistry, 27:5308–14.
34. Tosteson MT, Tosteson DC. (1981). The sting melittin forms channels in lipid bilayers. Biophys J, 36:109–16.
35. Vogel H, Jahnig F. (1986). The structure of melittin in membranes. Biophys J, 50:573–82.
36. Benachir T, Lafleur M. (1995). Study of vesicle leakage induced by melittin. Biochim Biophys Acta, 1235:452–60.
37. Pawlak M, Meseth U, Dhanapal B. (1994). Template-assembled melittin: Structural and functional characterization of a designed, synthetic channel forming protein. Protein Sci, 3:1788–805.
38. Räder K, Wildfeuer A, Wintersberger F, Bossinger P, Mücke HW. (1987). Characterization of bee venom and its main components by high performance liquid chromatography. J Chromatogr, 408:341–8.
39. Lowry OH, Rosebrough N J, Farr AL, Randall RL. (1951). Protein measurement with the Folin phenol reagent. J Biol Chem, 193:265–75.
40. Sah H. (1997). A new strategy to determine the actual protein content of poly (lactide-co-glycolide) microspheres. J Pharm Sci, 86:1315–8.
41. Gevod VS, Birdi KS. (1984). Melittin and the 8–26 fragment. Differences in ionophoric properties as measured by monolayer method. Biophys J, 45:1079–83.
42. Terwillinger TC, Eisenberg D. (1982). The structure of melittin. 2. Interpretation of the structure. J Biol Chem, 257:6016–22.
43. Meek JL, Rossettio ZL. (1981). Factors affecting retention and resolution of peptides in high performance liquid chromatography. J Chromatogr, 211:15–28.
44. Hegg PO. (1979). Precipitation of egg white proteins below their isoelectric points by sodium dodecyl sulfate and temperature. Biochim Biophys Acta, 579:73–87.
45. Bello J, Bello HR, Granados E. (1982). Conformation and aggregation of melittin: Dependence on pH and concentration. Biochemistry, 21:461–5.
46. Sessa G, Freer JH, Colacicco G, Weismann G. (1969). Interaction of a lytic polypeptide, melittin, with lipid membrane systems. J Biol Chem, 244:3575–82.
47. Choi SH, Park TG. (2000). Hydrophobic ion pair formation between leuprolide and sodium oleate for sustained release from biodegradable polymeric microspheres. Int J Pharm, 203:193–202.
48. Yoo HS, Park TG. (2004). Biodegradable nanoparticles containing protein–fatty acid complexes for oral delivery of salmon calcitonin. J Pharm Sci, 93:488–95.
49. Akyü S, Severcan F. (1988). Melittin–lipid interactions: A FT-IR spectroscopic study. J Mol Struct, 175:371–6.
50. Dorkoosh FA, Verhoef JC, Ambagts MHC, Rafiee-Tehrani M, Borchard G, Junginger HE. (2002). Peroral delivery systems based on superorous hydrogel polymer: Release characteristics for the peptide drugs buserelin, octreotide and insulin. Eur J Pharm Sci, 15(5):433–9.
51. Gaikar VG, Padalkar KV, Aswal VK. (2008). Characterization of mixed micelles of structural isomers of sodium butyl benzene sulfonate and sodium dodecyl sulfate by SANS, FTIR spectroscopy and NMR spectroscopy. J Mol Liq, 138(1–3):155–67.
52. Haris PI, Chapman D. (2004). Analysis of polypeptide and protein structures using Fourier transform infrared spectroscopy. Methods Mol Biol, 22:183–202.
53. Yang H, Yan X-H, Wang Z-L, Cheng R-S. (2001). The crystallizing behavior of sodium dodecyl sulfate under a electrostatic field. Chem J Chinese Universities, 22:666–8.

54. Sun SP, Cui FD, Kawashima Y, Liang N, Zhang LQ, Shi K, et al. (2008). A novel insulin–sodium oleate complex for oral administration: Preparation, characterization and in vivo evaluation. J Drug Del Sci Tech, 18(4):239–43.
55. Brandts JF, Hunt L. (1967). The thermodynamics of protein denaturation. III. The denaturation of ribonuclease in water and in aqueous urea and aqueous ethanol mixture. J Am Chem Soc, 89:4826–38.
56. Pace CN. (1975). The stability of globular proteins. CRC Crit Rev Biochem, 3(1):1–43.
57. Boye JI, Ma CY, Ismail A. (2004). Thermal stability of beta-lactoglobulins A and B: Effect of SDS, urea, cysteine and *N*-ethylmaleimide. J Dairy Res, 71(2):207–15.
58. Lengsfeld CS, Pitera D, Manning M, Randolph TW. (2002). Dissolution and partitioning behavior of hydrophobic ion-paired compounds. Pharm Res, 19:1572–6.
59. Kendrick BS, Meyer JD, Matsuura JE, Carpenter JF, Manning MC. (1997). Hydrophobic ion pairing as a method for enhancing structure and activity of lyophilized subtilisin BPN' suspended in isooctane. Arch Biochem Biophys, 347:113–8.
60. Cui FD, Shi K, Zhang LQ, Tao AJ, Kawashima Y. (2006). Biodegradable nanoparticles loaded with insulin–phospholipid complex for oral delivery: Preparation, in vitro characterization and in vivo evaluation. J Control Release, 114:242–50.